Journal of Sound and Vibration (2001) **245**(4), 611–631
doi:10.1006/jsvi.2001.3596, available online at http://www.idealibrary.com on IDEAL®

APPROXIMATE MODELLING OF FLUID INFLUENCE ON AXISYMMETRIC WAVE DISPERSION IN AN INFINITE HOLLOW CYLINDER

T. MAZÚCH

Institute of Materials and Machine Mechanics, Slovak Academy of Sciences, Department of FEM, Branch Martin, Severná 14, *SK* - 036 80 *Martin, Slovakia. E-mail: tiborm@savmt.sk*

(*Received* 2 *March* 2000, *and in final form* 8 *December* 2000)

The dispersion of the axisymmetric stress waves propagated in the infinite hollow cylinder filled with water is studied. Modification of a semianalytical FE approach for "dry" cylinders for this case and other independent FE approaches are described. The usage of the approaches in question is demonstrated for thick and thin cylinders in cases of isotropic and composite (monoclinic) materials. Influence of water upon the dispersion properties of waves is demonstrated by dispersion curves and shapes of waves. Some dispersion curves were influenced by fluid only weakly, but some dispersion curves were influenced very strongly even for very thick cylinders.

1. INTRODUCTION

The problem of propagation of harmonic stress waves in hollow cylinders has been intensively studied during the last few decades. The analytical and numerical approaches are concerned mainly with hollow, linearly elastic and anisotropic cylinders. Detailed reviews of the present state are given in references [1, 2]. Recently, a simple approach was suggested for obtaining finite elements for modelling the dispersion of stress waves [3] propagated in anisotropic, linearly elastic bodies of infinite length with cross-section of arbitrary shape, but constant lengths along the body. The approach allows one to model a given problem without using the so-called (semi)infinite elements.

The aim of this paper is modelling the above-mentioned problem for the case when the hollow cylinder is filled with water: i.e., investigating the influence of this fluid on the dispersion curves. For this purpose, a simplified model of the fluid has been chosen, used successfully in references [4, 5], where the influence of ideal fluid on the natural vibration of a thin cylindrical shell (clamped at one end, and free at the other end) was investigated. The suitability of using this model is evident from the excellent agreement of FEM calculations with experiments for the case of a simple shell, filled gradually with fluid [4], as well as for the case, when fluid was in the cylindrical annulus between the elastic wall and the perfectly rigid wall, for various widths of the annulus [5]. For a verification of the semianalytical results, another finite element approach is used in this paper.

2. MODEL USED OF FLUID AND FEM FORMULATION

For the simplified model of incompressible and inviscid fluid it is assumed that the amplitude of the pressure satisfies the Laplace equation

$$\Delta p(x, r) = 0 \tag{1}$$

0022-460X/01/340611 + 21 $35.00/0

and a boundary condition

$$\frac{\mathrm{D}p}{\mathrm{d}n} = -\rho_f \frac{\partial^2 w(x, r, t)}{\partial t^2} \quad \text{on } A_C, \tag{2}$$

where A_c is the common fluid structure interface, n is a co-ordinate taken along the normal, ρ_f is the fluid density and w is the structural radial displacement. This model in connection with FEM was used by Zienkiewicz *et al.* for the first time in 1965 [6]. Equation (1) and the boundary condition (2) can be replaced by equivalent variational formulations, given in reference [7] for example.

For the given problem it is supposed that the solution is of the form

$$p(r, x, t) = P(r)\cos[\xi(x \pm ct)], \quad u(r, x, t) = U(r)\sin[\xi(x \pm ct)],$$

$$v(r, x, t) = V(r)\cos[\xi(x \pm ct)], \quad w(r, x, t) = W(r)\cos[\xi(x \pm ct)], \tag{3}$$

where p is the fluid pressure, u, v and w are longitudinal, circumferential and radial displacements of the elastic cylinder, c is the phase velocity of the axisymmetric wave, $\xi = 2\pi/\Lambda$, Λ is the wavelength and t is the time. Upon considering the strain vector for the three-dimensional axisymmetric case (see reference [8] for example)

$$\varepsilon = \begin{Bmatrix} \partial u/\partial x \\ w/r \\ \partial w/\partial r \\ \partial v/\partial r - v/r \\ \partial w/\partial x + \partial u/\partial r \\ \partial v/\partial x \end{Bmatrix} \tag{4}$$

and the elasticity matrix in the form

$$\mathbf{E} = \begin{bmatrix} e_{11} & e_{12} & e_{13} & e_{14} & 0 & 0 \\ e_{21} & e_{22} & e_{23} & e_{24} & 0 & 0 \\ e_{31} & e_{32} & e_{33} & e_{34} & 0 & 0 \\ e_{41} & e_{42} & e_{43} & e_{44} & 0 & 0 \\ 0 & 0 & 0 & 0 & e_{55} & e_{56} \\ 0 & 0 & 0 & 0 & e_{65} & e_{66} \end{bmatrix}, \tag{5}$$

this approach gives the generalized eigenvalue problem in the form

$$\Lambda^2 \mathbf{K}(\Lambda)\mathbf{w}_i = (2\pi c_i)^2[\mathbf{M} + \mathbf{M}_D(\Lambda)]\mathbf{w}_i, \tag{6}$$

where $\mathbf{K}$ and $\mathbf{M}$ are the *in vacuo* structural wave global stiffness and mass matrices derived early in reference [3]. These are in the form

$$\mathbf{K}_e(\Lambda) = 2\pi \int_{R_1}^{R_2} \mathbf{B}^{\mathrm{T}}\mathbf{E}\mathbf{B}r\,\mathrm{d}r, \quad \mathbf{B} = [\mathbf{B}_1, \mathbf{B}_2, \ldots, \mathbf{B}_q], \tag{7}$$

where R_1, R_2 are inner and outer radius, q is the number of the element nodal points,

$$\mathbf{B}_k^{\mathrm{T}} = \begin{bmatrix} 2\pi N_u, & 0, & 0, & 0, & \Lambda \dfrac{\partial N_u}{\partial r}, & 0 \\ 0, & 0, & 0, & -\Lambda \dfrac{N_v}{r} + \Lambda \dfrac{\partial N_v}{\partial r}, & 0, & -2\pi N_v \\ 0, & \dfrac{\Lambda}{r} N_w, & \Lambda \dfrac{\partial N_w}{\partial r}, & 0, & -2\pi N_w, & 0 \end{bmatrix} \tag{8}$$

and N_u, N_v and N_w are shape functions for approximations $U(r)$, $V(r)$ and $W(r)$. The mass matrix element is in the form

$$\mathbf{M}_e = 2\pi\rho \int_{R_1}^{R_2} \mathbf{H}^{\mathrm{T}}\mathbf{H} r \, \mathrm{d}r, \quad \mathbf{H} = [\mathbf{H}_1, \mathbf{H}_2, \ldots, \mathbf{H}_q] \tag{9}$$

with the submatrices of the matrix $\mathbf{H}$

$$\mathbf{H}_k = \begin{bmatrix} N_u, & 0, & 0 \\ 0, & N_v, & 0 \\ 0, & 0, & N_w \end{bmatrix}. \tag{10}$$

The matrix

$$\mathbf{M}_D = \rho_f \mathbf{S}^{\mathrm{T}} \mathbf{K}_f^{-1} \mathbf{S} \tag{11}$$

is the so-called added mass matrix. Derivation of such a (reduced) mass matrix was first suggested by Zienkiewicz *et al.* [6]. $\mathbf{S}$ and $\mathbf{K}_f$ are the global interaction and fluid stiffness matrices. The element of the wave stiffness matrix for the fluid can be expressed by

$$\mathbf{K}_{fe}(\Lambda) = 2\pi \int_0^{R_1} \mathbf{B}_f^{\mathrm{T}} \mathbf{B}_f r \, \mathrm{d}r, \quad \mathbf{B}_f = [\mathbf{b}_1, \mathbf{b}_2, \ldots \mathbf{b}_q] \tag{12}$$

with

$$\mathbf{b}_j = \begin{Bmatrix} 2\pi N_p \\ \Lambda \partial N_p / \partial r \end{Bmatrix}, \tag{13}$$

where N_p are shape functions for the pressure approximation. The global interaction matrix $\mathbf{S}$ for the axisymmetric case has only one non-zero element

$$s_{kl} = 2\pi \Lambda R_1 \tag{14}$$

in the position given by the kth row and the lth column corresponding with the pressure and the radial displacement at the interaction interface. The eigenvector $\mathbf{w}_i$ represents shape of the ith wave, with the phase velocity c_i. The phase velocities and the corresponding shapes of the waves are solved for the particular value of the wavelength Λ.

3. ALTERNATIVE FE APPROACH

This approach (used in reference [9] for the case of the cylinder *in vacuo*) is based on the assumption that the propagated waves and the standing waves have the same dispersion

properties. One can then use the analytical solution for the hollow cylinder simply supported at both ends

$$u_A = U_A(r)\cos\frac{m\pi x}{L}\cos\omega t, \quad v_A = V_A(r)\sin\frac{m\pi x}{L}\cos\omega t,$$

$$w_A = W_A(r)\sin\frac{m\pi x}{L}\cos\omega t, \tag{15}$$

where U_A, V_A and W_A are the functions sought, m is the number of half-waves in the longitudinal direction, ω is circular frequency and L is the length of the cylinder. The simple supporting of the hollow cylinder can be expressed by boundary conditions in the form

$$N_x = M_x = v_A = w_A = 0 \tag{16}$$

at $x = 0$ and L, where N_x is the normal force, M_x is the flexural moment and v_A, w_A are the circumferential and radial displacements. The natural modes of vibration of the cylinder are sinusoidal with the wavelength $\Lambda = 2L/m$. It is supposed that in the case of these boundary conditions, too dramatic differences between "dry" and "wet" eigenmodes cannot occur as have occurred in case of the clamped–free cylinder in reference [4]. Discretization of the hollow cylinder with respect to the boundary conditions (2) and (16) gives the generalized eigenvalue problem in the form

$$\mathbf{K}_A\mathbf{x}_i = \left(\frac{\pi m c_{ieqv}}{L}\right)^2(\mathbf{M}_A + \mathbf{M}_{AD})\mathbf{x}_i, \tag{17}$$

where $\mathbf{K}_A$ is the symmetric, sparse and positive semi-definite (due to boundary conditions) global stiffness matrix, $\mathbf{M}_A$ is the symmetric, sparse and positive-definite global mass matrix and $\mathbf{M}_{AD}$ is the added mass matrix given by

$$\mathbf{M}_{AD} = \rho_f \mathbf{S}_A^{\mathrm{T}}\mathbf{K}_{Af}^{-1}\mathbf{S}_A. \tag{18}$$

Note that the interaction matrix $\mathbf{S}_A$ has a more complicated form than the matrix $\mathbf{S}$ in the previous case. c_{ieqv} is the ith equivalent standing wave phase velocity and $\mathbf{x}_i$ is the corresponding eigenvector representing the ith natural mode of vibration. This system has one rigid-body mode in axial direction and its first eigenfrequency is zero. The lowest eigenpairs of equation (17) cannot be effectively solved by a standard manner based on the vector iterations. The problem with the singular stiffness matrix and the full (not sparse) added mass matrix can be avoided by using an incomplete modal decomposition of the *in vacuo* system,

$$\mathbf{X}_R^{\mathrm{T}}\mathbf{K}_A\mathbf{X}_R = \Lambda_R, \quad \mathbf{X}_R^{\mathrm{T}}\mathbf{M}_A\mathbf{X}_R = \mathbf{I}_R \tag{19}$$

for the transformation into the reduced form

$$\Lambda_R\mathbf{y}_{Ri} = \mu_i^2(\mathbf{I}_R + \mathbf{X}_R^{\mathrm{T}}\mathbf{M}_{AD}\mathbf{X}_R)\mathbf{y}_{Ri}. \tag{20}$$

Then, for the approximation of the eigenpairs of the generalized eigenvalue problem (17) one can write

$$\mu_i \cong \frac{\pi m c_{ieqv}}{L}, \quad \mathbf{x}_i \cong \mathbf{X}_R\mathbf{y}_i. \tag{21}$$

This approach gives the upper approximations of the equivalent standing wave phase velocities. Note that the explicit construction of the full added mass matrix used in equation (20) can be avoided by using the Cholesky decomposition of the global fluid stiffness matrix.

4. NUMERICAL EXAMPLES

The approach described can be applied to the case of investigation of the influence of ideal fluid (water with density $\rho_f = 1000\ \mathrm{kg/m^3}$ was considered) on phase velocities and shapes of the waves in the infinite hollow thick cylinders. The ratios of the outer to inner radius of the cylinders were taken to be $R_2/R_1 = 1{\cdot}50$ and $R_2/R_1 = 1{\cdot}05$. It should be noted that $R_1 = 1\ \mathrm{m}$ was used in the calculations. Two cases of the material were taken into account.

(1) *Isotropic—steel* with the Poisson ratio $\mu = 0{\cdot}29$. For the solution of the phase velocities Young's modulus $E = 2{\cdot}05 \times 10^{11}$ Pa and mass density $\rho = 7800\ \mathrm{kg/m^3}$ were considered.

(2) *Composite—unidirectional boron epoxy* [10] with the fiber direction 60° with respect to the x-axis: i.e., material with *monoclinic symmetry*. The elements of the elasticity matrix

$$\mathbf{E} = 6{\cdot}89475 \times 10^9 \begin{bmatrix} 18{\cdot}86949079 & 5{\cdot}83728780 & 0{\cdot}97118634 & -8{\cdot}68814264 & 0 & 0 \\ 5{\cdot}83728780 & 5{\cdot}23220320 & 0{\cdot}87966097 & -3{\cdot}12209485 & 0 & 0 \\ 0{\cdot}97118634 & 0{\cdot}87966097 & 3{\cdot}23389825 & -0{\cdot}07926329 & 0 & 0 \\ -8{\cdot}68814264 & -3{\cdot}12209485 & -0{\cdot}07926329 & 6{\cdot}32033879 & 0 & 0 \\ 0 & 0 & 0 & 0 & 1{\cdot}275 & 0{\cdot}38971143 \\ 0 & 0 & 0 & 0 & 0{\cdot}38971143 & 0{\cdot}825 \end{bmatrix}$$

are given in Pa and the mass density $\rho = 2000\ \mathrm{kg/m^3}$ was used.

For the semianalytical FE formulation the finite element models of the cylinders and water consisted of 250 three-noded quadratic isoparametric finite wave elements and all finite element models used had 1503 degrees of freedom (d.o.f.s) for the elastic cylinder and 501 degrees of freedom for water. The Lanczos algorithm with simple orthogonalization [11] modified for the case of the added mass matrix was used for the generalized eigenvalue problem (6). For the alternative FE formulation, the finite element models of the cylinders and water consisted of 200 eight-noded quadratic isoparametric axisymmetric finite elements with 1899 degrees of freedom for the elastic cylinder and 661 degrees of freedom for water. For this approach, 40 *in vacuo* eigenpairs were used and the reduced eigenvalue problem (20) was solved by the Jacobi iteration method.

Two types of axisymmetric waves were considered for the isotropic material. Rotationally symmetric waves are characterized by $u(x, r, t) \neq 0$, $v = 0$ and $w(x, r, t) \neq 0$ and torsional waves by $u = w = 0$ and $v(x, r, t) \neq 0$. Torsional waves cannot be influenced by ideal fluid described by equations (1) and (2). Influence of water on the dispersion properties of rotationally symmetric waves is apparent in a decrease of calculated phase velocities. This influence is evident for dispersion curves of a thick cylinder, in Figure 1. Curves of "wet" dispersion approximate curves of "dry" curves well, and the phase velocities are influenced in most of cases only weakly. Somewhat greater differences appeared for longer waves for

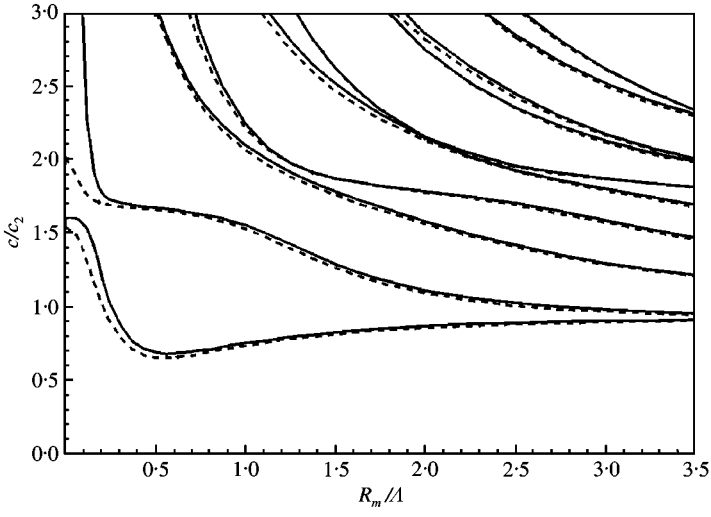

Figure 1. First 10 dispersion curves of rotationally symmetric waves propagated in a thick isotropic infinite hollow cylinder with $R_2/R_1 = 1{\cdot}50$ where c_2 is shear wavespeed in 3-D continuum; $R_m = (R_1 + R_2)/2$; Λ is wavelength; solid lines hold for "dry" cylinder; dashed lines hold for a cylinder filled with water.

the first (the lowest) dispersion curve (for $R_m/\Lambda < 0{\cdot}5$) and for the second curve (for $R_m/\Lambda < 0{\cdot}2$) where the decrease of phase velocities is suddenly expressive. Calculated phase velocities for $R_m/\Lambda = 0{\cdot}3125$ are shown in Table 1. For an exact solution of the phase velocities of rotationally symmetric waves and analytical solution of the phase velocities of torsional waves the known Pochhammer solutions for full "dry" cylinder [12, 13] has been modified by considering zero stresses at two surfaces of a hollow cylinder (see Appendices A and B). These solutions were executed by using the computer code Mathematica [14]. Comparison of these results with results achieved by the semianlytical FE approach shows an excellent agreement with the largest relative error $\varepsilon < 0{\cdot}001\%$. Agreement between both FE approaches is acceptable both for the "dry" and "wet" cylinders. Some of the calculated shapes of waves are shown in Figure 2. As was mentioned above, the shapes of the waves were solved as eigenvectors of problem (6). For better illustration, these shapes are shown as obtained by using the 2-D elements and also (for $x = \text{const.}$) by using their components $u(r)$ and $w(r)$. Norms used for the eigenvectors are evident from the figure. Although the first phase velocity decreased by about more than 9%, the change of corresponding wave shape appears only in a very small shift of the nodal circle (with respect to the inner surface). In contradiction to "dry" wave shape, the nodal circle of the radial displacements appears in the "wet" shape of the second wave. The fluid influence on the third wave shape appeared in the small decrease of the radial displacements. Somewhat greater differences have appeared in locations of nodal circles of axial and radial displacements for fourth wave shape, as well as a larger decrease of axial displacements.

From Figure 2 one can see that the magnitude of a decrease of the phase velocities depends on relative magnitudes (further RM) of the radial displacements at the inner surface of the "dry" cylinder (i.e. at $r = R_1$). In cases where RM of these displacements are dominant (see the first and fourth "dry" wave shapes), a decrease is significant even for a very thick cylinder. If RM of radial displacements at inner surface are small and RM of axial displacements there are dominant, the decrease of phase velocities is small (see the second and third wave shapes). This statement holds only for those cases where "wet"

TABLE 1(a)

The computed phase velocities of the rotationally symmetric waves in the infinite thick isotropic cylinder for $R_m/\Lambda = 0{\cdot}3125$

	"Dry" (empty) cylinder			"Wet" cylinder (filled with water)	
		Finite element method		Finite element method	
i	Exact (modified Pochhammer) c_{ei} (m/s)	Semianalytical (Mazúch) c_{1i} (m/s)	Alternative c_{2i} (m/s)	Semianalytical (Mazúch) c_{3i} (m/s)	Alternative c_{4i} (m/s)
1	2738·61	2738·62	2738·62	2484·94	2486·09
2	5422·87	5422·88	5422·88	5357·43	5358·67
3	14109·8	14109·83	14109·93	13915·86	13949·27
4	22758·3	22758·30	22759·05	19132·96	19160·14
5	27082·4	27082·42		26188·56	
6	38284·8	38284·85		38004·10	
7	47479·0	47479·01		40617·80	
8	51168·7	51168·68		51167·64	
9	63951·2	63951·18		62126·64	
10	70657·2	70657·29		63965·94	
11	76751·9	76751·90		76688·65	
12	89367·3	89367·34		84742·78	

TABLE 1(b)

The computed phase velocities of the torsional waves in the infinite thick isotropic cylinder for $R_m/\Lambda = 0{\cdot}3125$

		Finite element method	
i	Analytical (modified Pochhammer) c_{ai} (m/s)	Semianalytical (Mazúch) c_{5i} (m/s)	Alternative c_{6i} (m/s)
1	3191·68	3191·68	3191·69
2	13536·6	13536·59	13536·68
3	25930·7	25930·68	
4	38566·6	38566·63	
5	51267·2	51267·19	
6	63994·0	63994·03	
7	76734·1	76734·12	
8	89481·8	89481·79	

dispersion curve approximates its "dry" curve well. In other cases, the situation is more complicated.

Results for a thin isotropic cylinder are shown in Figures 3 and 4 and in Table 2. Some dispersion curves (see third, sixth and eighth curve in Figure 3) and great part of second curve (for $R_m/\Lambda > 0{\cdot}3$) were influenced only weakly. Moreover, fourth and seventh curves were influenced strongly even for shorter wavelengths. Similarly, as for the thick cylinder, the first curve for $R_m/\Lambda < 0{\cdot}7$ and second curve for $R_m/\Lambda < 0{\cdot}2$ are influenced quite dramatically. Computed phase velocities for $R_m/\Lambda = 0{\cdot}5125$ are shown in Table 2. An excellent agreement between Pochhammer solutions and finite element approaches and

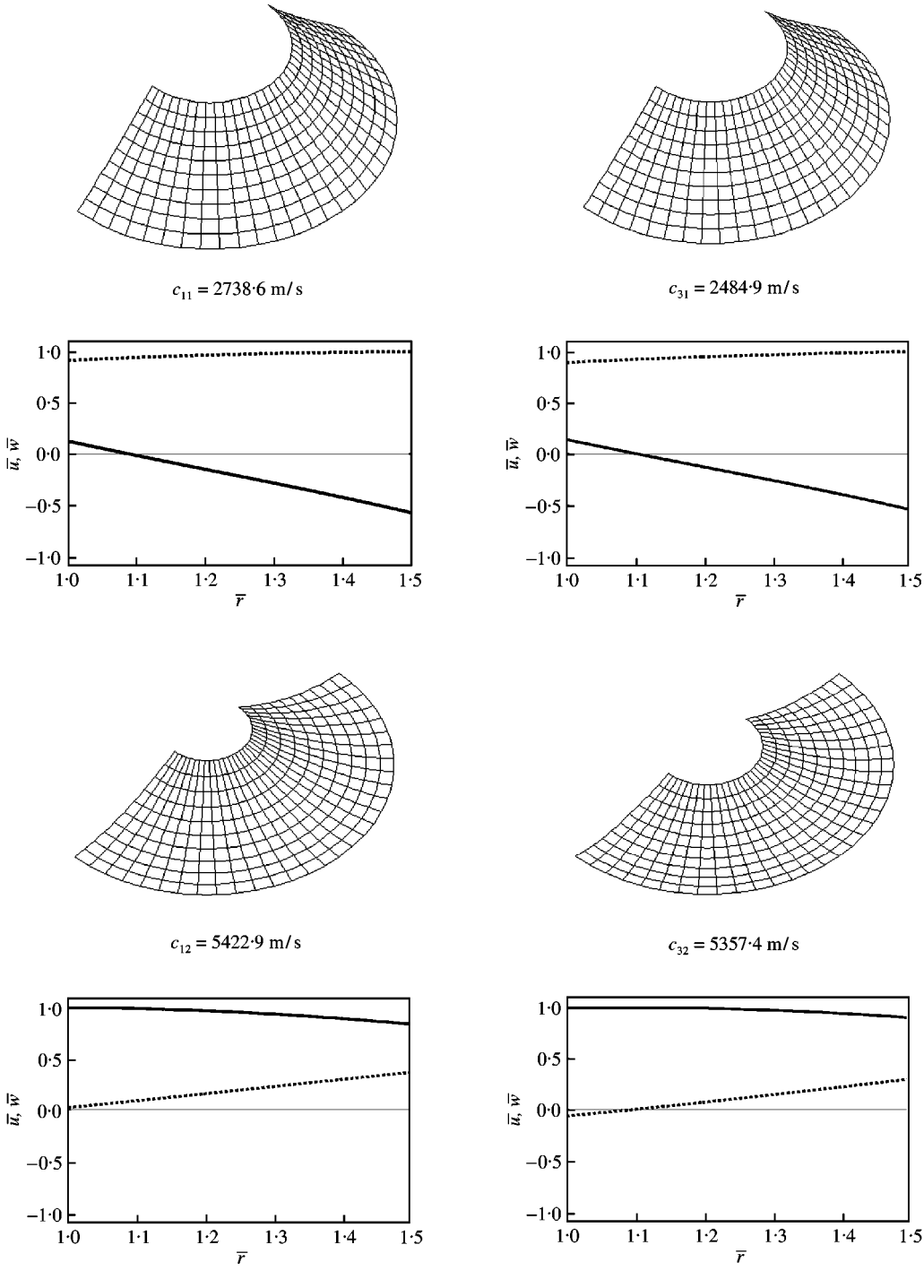

Figure 2. First four computed shapes of rotationally symmetric waves for Table 1. Left—"dry" cylinder, right—cylinder filled with water; top—image by using 2-D elements, bottom—normed displacements (—— lines hold for axial $\bar{u}$ and ..... lines for radial displacements $\bar{w}$; $\bar{r} = r/R_1$—dimensionless radius).

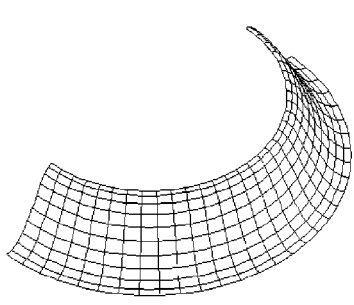

c_{13} = 14 109·8 m/s

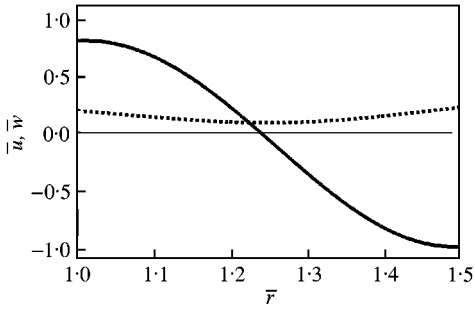

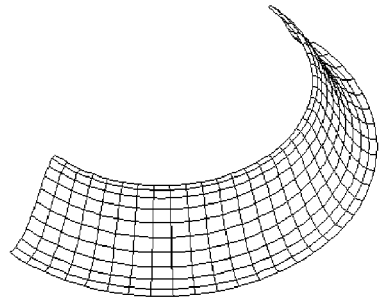

c_{33} = 13 915·9 m/s

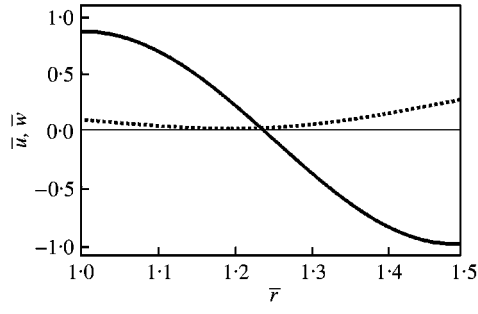

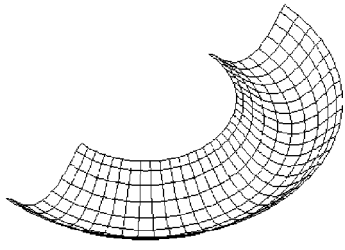

c_{14} = 22 758·3 m/s

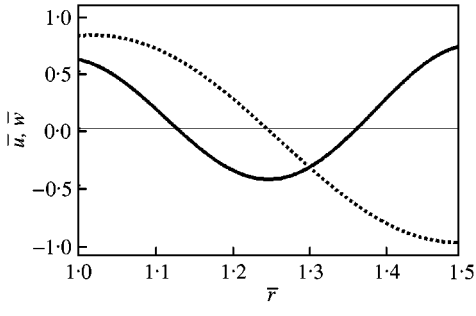

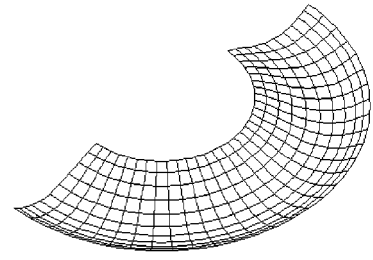

c_{34} = 19 133·0 m/s

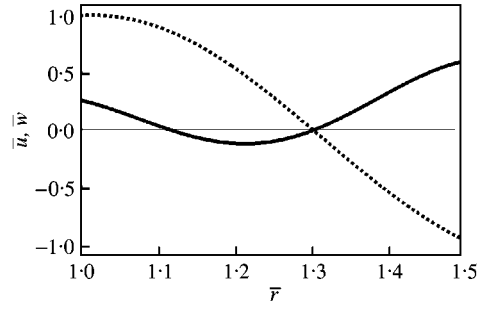

Figure 2. Continued.

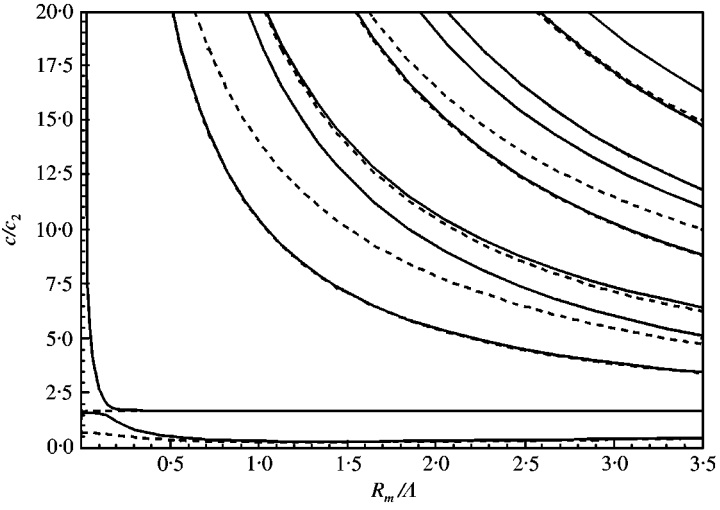

Figure 3. First 10 dispersion curves of rotationally symmetric waves propagated in a thin isotropic infinite hollow cylinder with $R_2/R_1 = 1{\cdot}05$, where c_2 is shear wavespeed in 3-D continuum; $R_m = (R_1 + R_2)/2$; Λ is wavelength; —— lines hold for "dry" cylinder; ---- lines hold for a cylinder filled with water.

also between both FE approaches in the "dry" and "wet" cases has been obtained. From Figure 4 it is evident that shapes of "dry" cylinder waves are appreciably changing with change of the parameter R_m/Λ. There are dominant radial displacements in the first wave shape (corresponding to the lowest dispersion curve), while in the second wave shape axial displacements are dominant, when shorter waves with $R_m/\Lambda = 0{\cdot}5125$ are considered. For longer waves characterized by $R_m/\Lambda = 0{\cdot}1025$ it is *vice versa*. Comparison of "dry" and "wet" shapes for shorter waves shows that although the first wave phase velocity decreases appreciably, the corresponding wave shape is influenced only minimally. In the second wave shape one can see only a small decrease of RM of radial displacements. A more interesting situation is the case of longer waves: i.e., for $R_m/\Lambda = 0{\cdot}1025$. In this case, the "wet" wave shape with dominant radial displacements corresponds to the first "dry" wave shape with dominant axial displacements. On the other hand, the predominantly axial "wet" wave shape corresponds to the second "dry" wave shape where radial displacements are dominant. This phenomenon has appeared although the dispersion curves do not cross each other. Similarity of the second "wet" wave shape and the first "dry" wave shape is probably caused by the fact that the second "wet" curve (for $R_m/\Lambda < 0{\cdot}2$) has become "disloyal" to the second "dry" curve and inclined towards the first "dry" curve.

In the case of composite monoclinic material, on the contrary to isotropic cylinders, axisymmetric waves are not separated into purely torsional and purely rotationally symmetric waves. These waves have all three components of displacements (axial, circumferential and radial) non-zero, so that all dispersion curves were influenced by contact with fluid. Results for thick monoclinic cylinder are shown in Figures 5 and 6 and in Table 3. Note, that in general, the decrease of phase velocities caused by contact with fluid is now greater than the decrease of phase velocities in the case of the isotropic thick cylinder (see Figure 1). Considering the thickness, this decrease is unexpectedly expressive. Calculated phase velocities for $R_m/\Lambda = 0{\cdot}3125$ are in Table 3. In the case of "dry" cylinder, agreement between both FE approaches is excellent, and for the "wet" cylinder agreement is acceptable. Somewhat greater differences appeared in this case and were probably caused

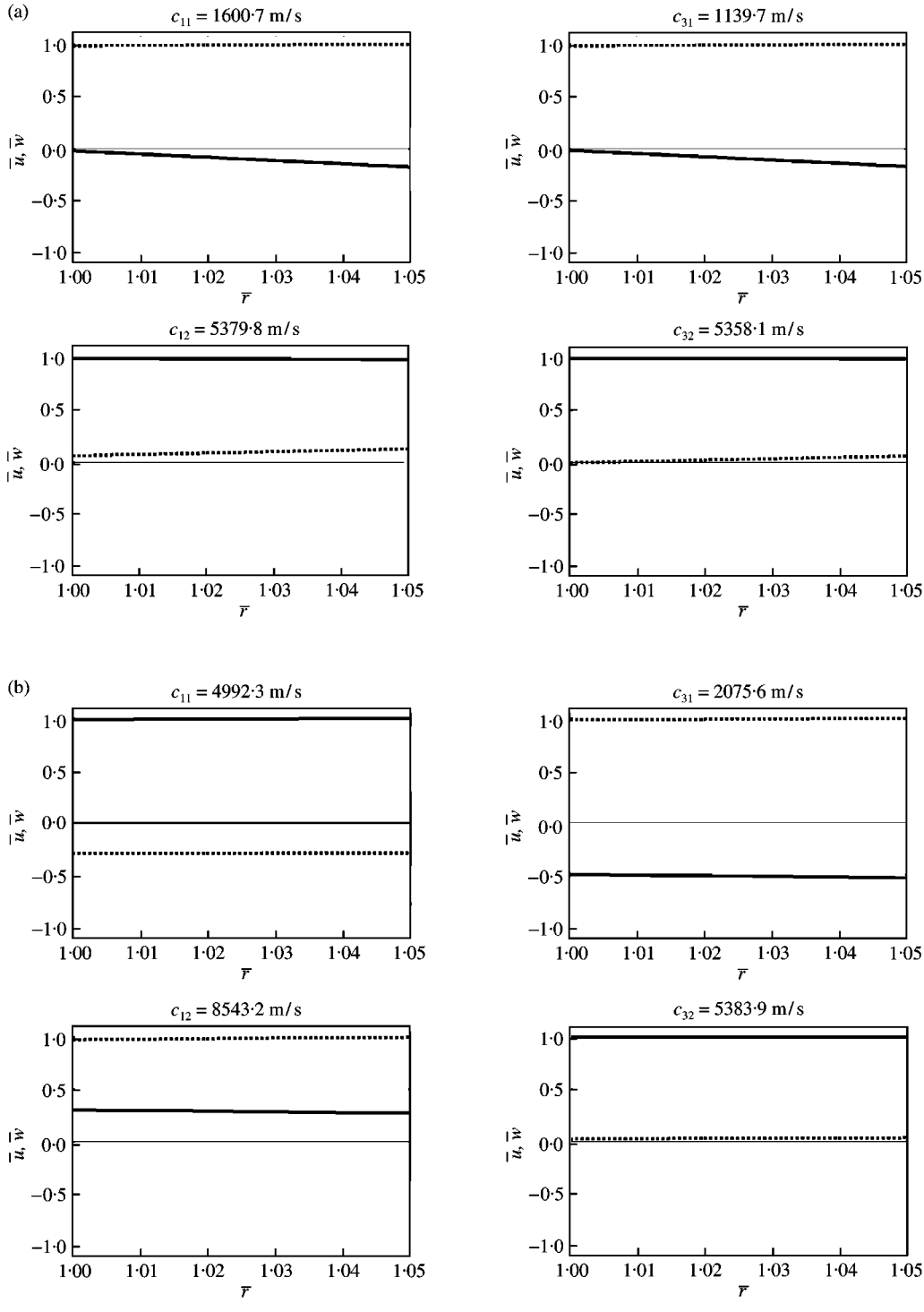

Figure 4. First two computed shapes of rotationally symmetric waves propagated in a thin isotropic cylinder imaged by using normed displcements: (a) for Table 2, i.e., $R_m/\Lambda = 0{\cdot}5125$, (b) for the $R_m/\Lambda = 0{\cdot}1025$; left—"dry" cylinder, right—cylinder filled with water; —— lines hold for axial $\bar{u}$ and ..... lines for radial displacements $\bar{w}$; $\bar{r} = r/R_1$-dimensionless radius.

TABLE 2(a)

The computed phase velocities of the rotationally symmetric waves in the infinite thin isotropic cylinder for $R_m/\Lambda = 0{\cdot}5125$

	"Dry" (empty) cylinder			"Wet" cylinder (filled with water)	
		Finite element method		Finite element method	
i	Exact (modified Pochhammer) c_{ei} (m/s)	Semianalytical (Mazúch) c_{1i} (m/s)	Alternative c_{2i} (m/s)	Semianalytical (Mazúch) c_{3i} (m/s)	Alternative c_{4i} (m/s)
1	1600·67	1600·67	1600·67	1139·67	1139·76
2	5379·78	5379·79	5379·80	5358·05	5358·12
3	64110·7	64110·72		63924·63	
4	117082·0	117082·07		75973·61	
5	128096·0	128095·63		127733·50	
6	191492·0	191492·07		183570·90	
7	234843·0	234843·32		191610·00	
8	255352·0	255352·21		255351·90	
9	319190·0	319189·69		298149·80	
10	352159·0	352159·41		319191·10	
11	383030·0	383030·40		383014·70	
12	446833·0	446833·70		414211·90	

TABLE 2(b)

The computed phase velocities of the torsional waves in the infinite thin isotropic cylinder for $R_m/\Lambda = 0{\cdot}5125$

	Analytical (modified Pochhammer)	Finite element method	
i	c_{ai} (m/s)	Semianalytical (Mazúch) c_{5i} (m/s)	Alternative c_{6i} (m/s)
1	3191·68	3191·68	3191·69
2	63942·2	63942·24	
3	127722·0	127721·7	
4	191537·0	191537·3	
5	255362·0	255361·9	
6	319190·0	319190·1	
7	383020·0	383020·2	
8	446851·0	446851·3	

by the fact that only the 40 lowest "dry" eigenpairs were substituted into equation (20). Calculated shapes of waves corresponding to Table 3 are depicted in Figure 6. Similarly, as in the case of a thin isotropic cylinder, interchange of shapes corresponding to the two lowest phase velocities is evident. In this case (see again the Figure 5 for $0{\cdot}2 < R_m/\Lambda < 0{\cdot}4$), deviation of the second "wet" curve relative to the first "dry" curve is evident while the first "wet" curve imitates a course of the second "dry" curve. Changes in the third wave shape, with dominant axial and expressive circumferential displacements, can be characterized by considerable shift of radial displacements nodal circle towards the outer surface. Evident

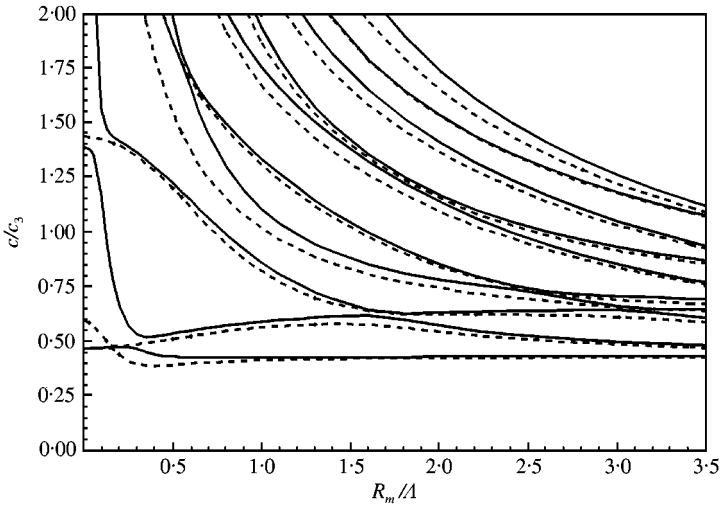

Figure 5. First 10 dispersion curves of axisymmetric waves propagated in a thick anisotropic infinite hollow cylinder with $R_2/R_1 = 1{\cdot}50$, where $c_3 = \sqrt{e_{33}/\rho}$; e_{33} is the diagonal element of the elasticity matrix; ρ cylinder mass density; $R_m = (R_1 + R_2)/2$; Λ the wavelength; —— lines hold for "dry" cylinder; ---- lines hold for a cylinder filled with water.

relationship exists between the fourth "dry" and fifth "wet" wave shapes. Similarly, as in the case of a thick isotropic cylinder, one can consider a relationship between the RM of radial displacements of "dry" wave shape at inner cylinder surface and between phase velocity of a "wet" wave having similar shape. In the case of "dry" wave shapes, where these RM of radial displacements are small, phase velocities corresponding to similar "wet" shapes are only slightly changed (see, e.g., a pair of wave shapes corresponding to the velocities c_{13} and c_{33}). In these cases, one cannot speak about decrease of phase velocities only, because in cases characterized by pairs of the velocities (c_{11}, c_{32}) and (c_{14}, c_{35}) increases have occurred. Unlike the case mentioned above, if one considers a "dry" wave shape with dominant RM of radial displacements at inner surface, a decrease of the phase velocity corresponding with the similar "wet" wave shape is appreciable (see, e.g., a pair characterized by the velocities c_{12} and c_{31}).

Dispersion curves for a thin monoclinic cylinder are shown in Figure 7. Similarly, as in the case of a thin isotropic cylinder, some dispersion curves are influenced by fluid appreciably, even the first, fifth and eighth ones for shorter wavelengths. The third curve for $R_m/\Lambda < 0{\cdot}2$ is influenced quite dramatically too. However, the second curve and a great part of the third curve (for $R_m/\Lambda > 0{\cdot}2$) are influenced negligibly. Calculated phase velocities for the parameter $R_m/\Lambda = 0{\cdot}5125$ are shown in Table 4. Note that agreement between both FE approaches is very good. Some calculated shapes of waves for phase velocities from Table 4 are shown in Figure 8. Radial displacements are dominant in the first wave shapes. Although a dramatic decrease of the first phase velocity is encountered, differences between "dry" and "wet" wave shapes are negligible. The second wave shapes are characterized by almost purely circumferential displacements and in the third wave shapes axial displacements are dominant. There are also minimal differences between "dry" and "wet" wave shapes. Dramatic differences between wave shapes corresponding to the fourth phase velocities can be explained similarly as in the above case.

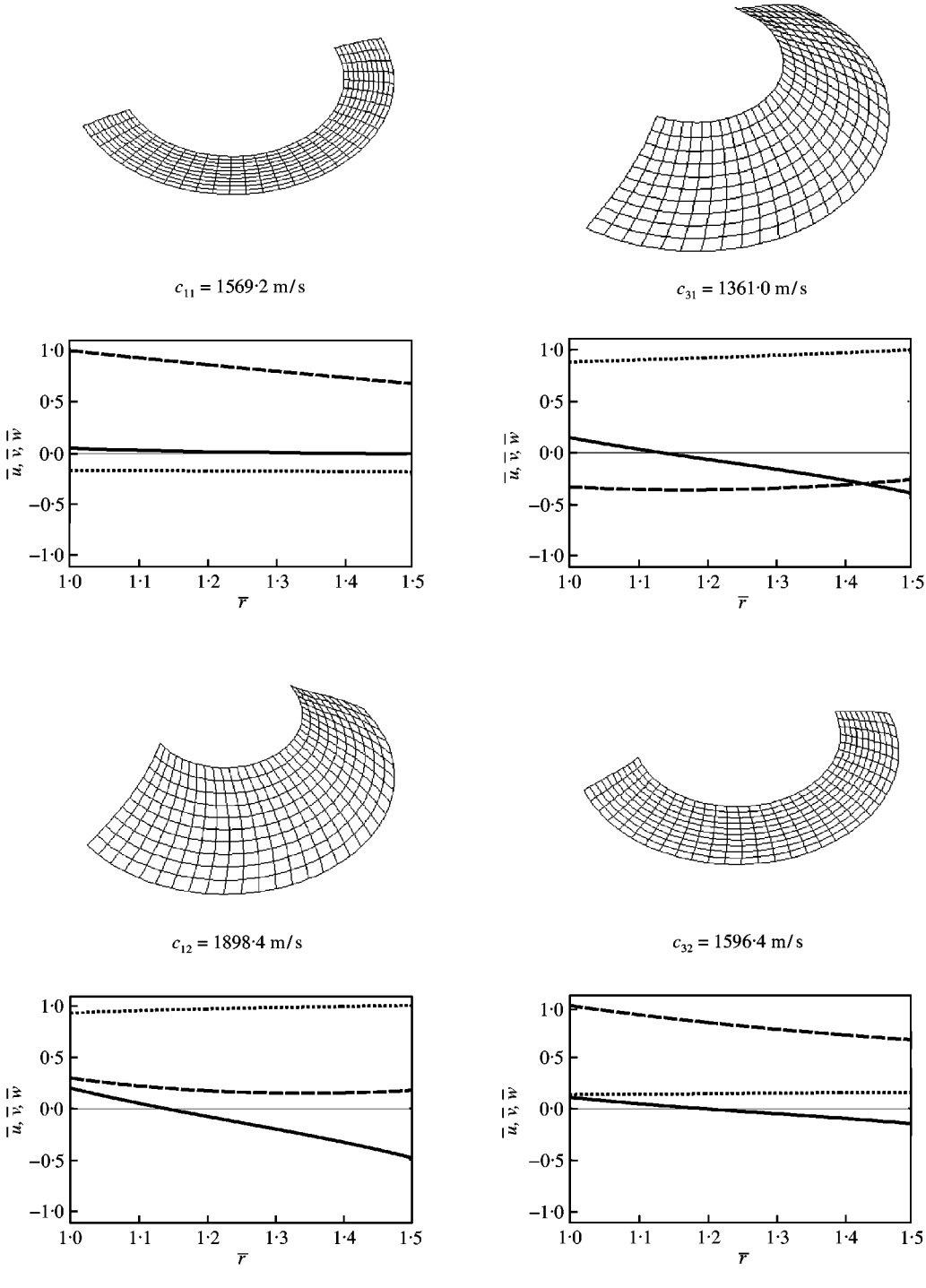

Figure 6. First five computed shapes of axisymmetric waves for Table 3. Left—"dry" cylinder, right—cylinder filled with water; top—image by using 2-D elements, bottom—normed displacements (—— lines hold for axial $\bar{u}$, ----- lines for circumferential $\bar{v}$ and ····· lines for radial displacements $\bar{w}$, $\bar{r} = r/R_1$—dimensionless radius).

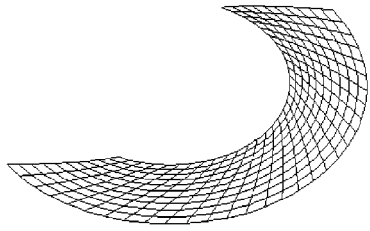

$c_{13} = 4630{\cdot}5$ m/s

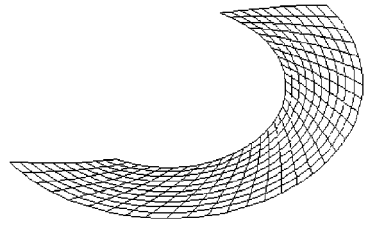

$c_{33} = 4570{\cdot}9$ m/s

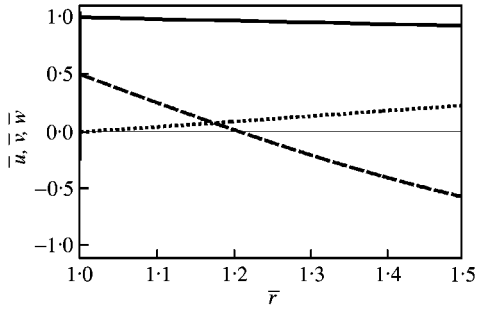

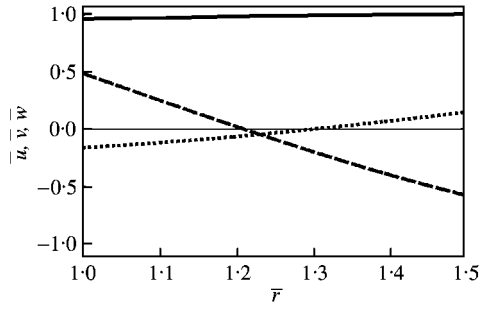

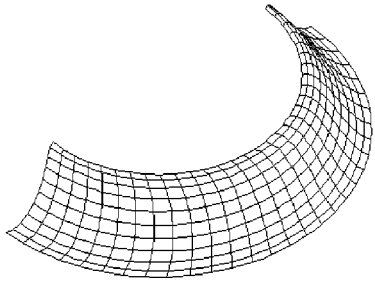

$c_{14} = 9755{\cdot}8$ m/s

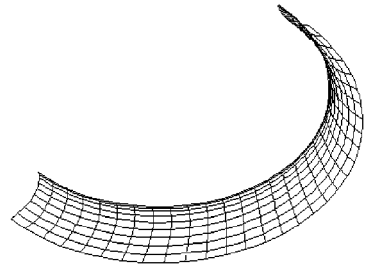

$c_{34} = 8327{\cdot}5$ m/s

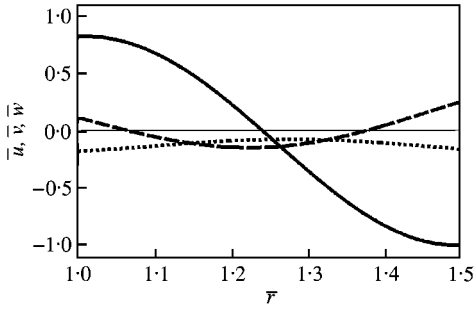

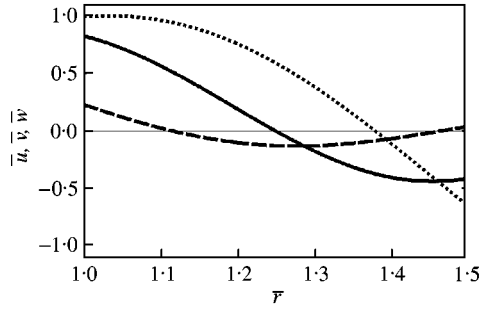

Figure 6. Continued.

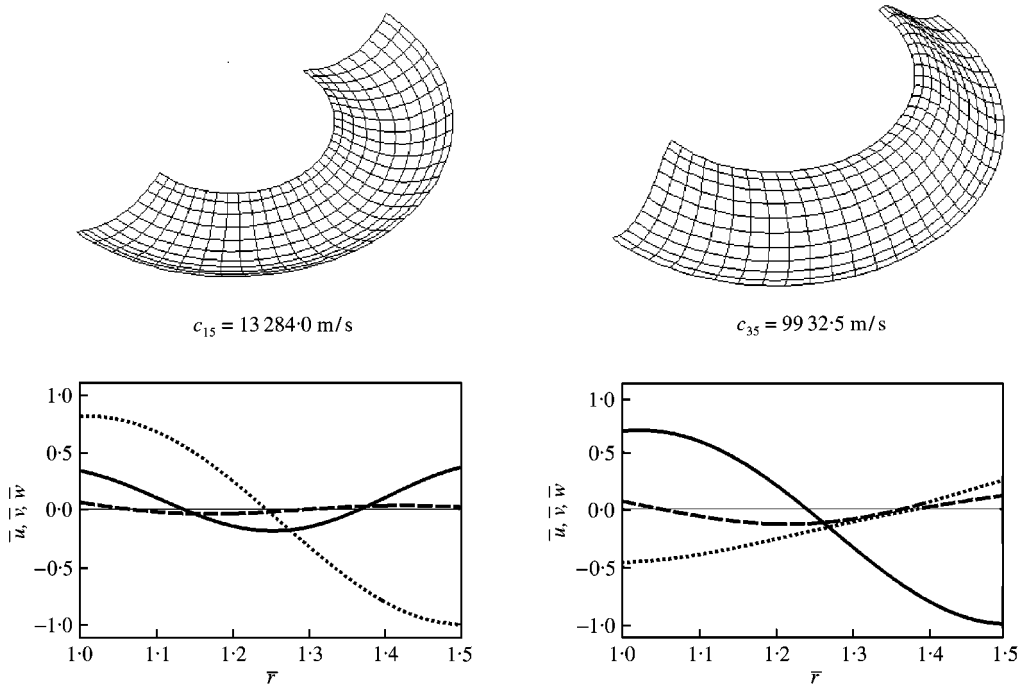

Figure 6. Continued.

TABLE 3

The computed phase velocities of the axisymmetric waves in the infinite thick monoclinic cylinder for $R_m/\Lambda = 0{\cdot}3125$

	"Dry" (empty) cylinder		"Wet" cylinder (filled with water)	
	Finite element method		Finite element method	
i	Semianalytical c_{1i}(m/s)	Alternative c_{2i}(m/s)	Semianalytical c_{3i}(m/s)	Alternative c_{4i}(m/s)
1	1569·22	1569·22	1361·03	1365·64
2	1898·36	1898·36	1596·40	1596·87
3	4630·45	4630·46	4570·91	4576·66
4	9755·77	9755·87	8327·48	8437·78
5	13284·04	13284·24	9932·48	10119·99
6	17326·37		16904·00	
7	20698·52		20694·13	
8	24965·63		21065·46	
9	27333·46		25404·41	
10	33659·04		33485·45	

5. CONCLUSIONS

Two approximate FE approaches for modelling the influence of water upon the dispersion properties of axisymmetric waves propagated in infinitely long hollow cylinder

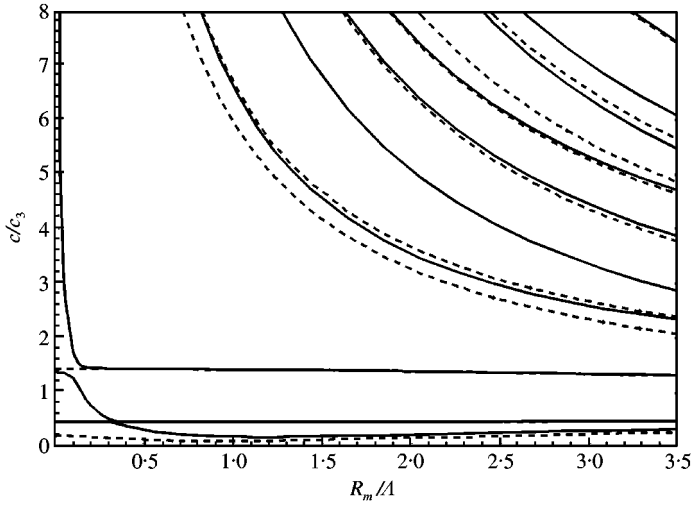

Figure 7. First 10 dispersion curves of axisymmetric waves propagated in a thin anisotropic infinite hollow cylinder with $R_2/R_1 = 1{\cdot}05$ where $c_3 = \sqrt{e_{33}/\rho}$; e_{33} is the diagonal element of the elasticity matrix; ρ the cylinder mass density; $R_m = (R_1 + R_2)/2$; Λ the wavelength; —— lines hold for "dry" cylinder; ---- lines for a cylinder filled with water.

TABLE 4

The computed phase velocities of the axisymmetric waves in the infinite thin monoclinic cylinder for $R_m/\Lambda = 0{\cdot}5125$

	"Dry" (empty) cylinder		"Wet" cylinder (filled with water)	
	Finite element method		Finite element method	
i	Semianalytical c_{1i}(m/s)	Alternative c_{2i}(m/s)	Semianalytical c_{3i}(m/s)	Alternative c_{4i}(m/s)
1	1051·59	1051·59	479·88	480·01
2	1561·24	1561·24	1561·21	1561·21
3	4805·48	4805·48	4792·10	4792·28
4	42235·46		36283·78	
5	66709·40		42352·45	
6	83939·79		83829·04	
7	93751·31		93720·10	
8	125724·4		101323·3	
9	133656·1		125834·6	
10	167742·6		167315·0	

have been presented. The semianalytical FE approach requires 1-D discretization only. For its independent verification an alternative FE approach with 2-D discretization has been used. Calculations by this approach lasted approximately 10 times longer (than for the semianalytical FE approach) and enable one to determine only a few dispersion curves. Moreover, that approach requires an additional time for manual or automatic identification of relevant eigenpairs (with $m = 1$). Comparison of the computed phase velocities by both FE approaches show very good agreement.

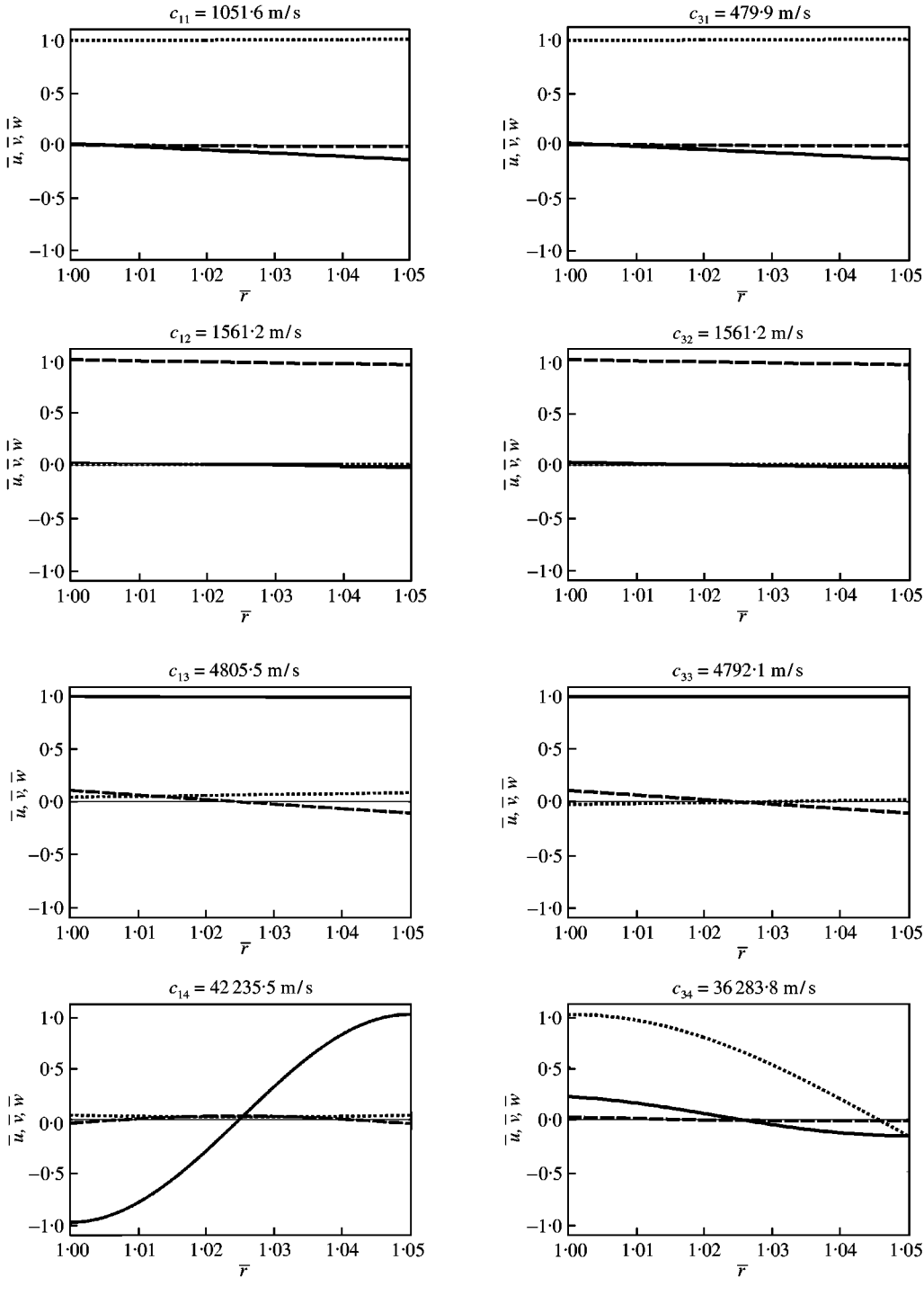

Figure 8. First four computed shapes of rotationally symmetric waves for Table 4 imaged by using normed displacements. Left—"dry" cylinder, right—cylinder filled with water; —— lines hold for axial $\bar{u}$; ---- lines for circumferential $\bar{v}$ and ····· lines for radial displacements $\bar{w}$, $\bar{r} = r/R_1$—dimensionless radius.

Only the rotationally symmetric waves were influenced by fluid in the case of the isotropic cylinder. In the case of the monoclinic material the purely torsional waves did not occur and all dispersion curves were influenced by fluid. A decrease of some phase velocities was negligible, but for some others it was unexpectedly appreciable even in the case of very thick cylinders. Influence of fluid upon shapes of waves is complicated and for a small vicinity of the considered parameter R_m/Λ, the following three possibilities occurred: (1) if "wet" dispersion curve approximates a course of "dry" curve well, the corresponding shapes of waves conform to each other; (2) if the ith "wet" curve inclines to the $(i-1)$th "dry" curve, the corresponding "wet" wave shape is similar to the $(i-1)$-th "dry" wave shape; (3) if the ith "wet" curve imitates the $(i+1)$th "dry" curve, the corresponding "wet" wave shape looks like the $(i+1)$th "dry" wave shape.

ACKNOWLEDGMENT

This work was partly supported by The Grant Agency of the Slovak Republic, under Grant No. 2/5095/20.

REFERENCES

1. K. P. SOLDATOS 1994 *Applied Mechanics Review* **47**, 501–516. Review of three dimensional dynamic analyses of circular cylinders and cylindrical shells.
2. K. P. SOLDATOS and J. Q. YE 1994 *Journal of Acoustic Society of America* **96**, 3744–3752. Wave propagation in anisotropic laminated hollow cylinders of infinite extend.
3. T. MAZÚCH 1996 *Journal of Sound and Vibration* **198**, 429–438. Wave dispersion modelling in anisotropic shells and rods by the finite element method.
4. MAZÚCH, J. HORÁČEK, J. TRNKA and J. VESELÝ 1996 *Journal of Sound and Vibration* **193**, 669–690. Natural modes and frequencies of thin clamped-free steel cylindrical storage tank partially filled with water: FEM and measurement.
5. J. HORÁČEK, T. MAZÚCH and J. TRNKA 1997 *Mechanical Engineering* (*Strojnícky časopis*) **48**, 351–362. Natural vibration of a cylindrical shell containing water in a coaxial annular gap.
6. O. C. ZIENKIEWICZ, B. M. IRONS and B. NATH 1965 *Proceedings of the Symposium on Vibration in Civil Engineering*, *London*, April 1965. Natural frequencies of complex free or submerged structures by finite elements method.
7. A. KARANACHOS and I. ANTONIADIS 1988 *Journal of Sound and Vibration* **121**, 77–104. Symmetric variational principles and modal methods in fluid–structure interaction problems.
8. T. KOHL and S. K. DATTA 1992 *Journal of Composite Material* **26**, 661–682. Mode-coupling of waves in laminated tubes.
9. T. MAZÚCH 1999 *Journal of Composite Materials* **33**, 1390–1410. Variant finite element applications to axisymmetric wave dispersion of cylinders.
10. N. J. PAGANO 1974 *Composite Materials*, Vol. **2**, 23–45. New York and London: Academic Press. Exact moduli of anisotropic laminates.
11. T. MAZÚCH 1991 *Proceedings of the Sixth International Conference on Mathematical Methods in Engineering*, *Plzen*, *Czechoslovakia*, 27–31 May, **II**, 363–368. The Lanczos method with simple orthogonalization.
12. L. POCHHAMMER 1876 *Journ. f. reine und angew. Mathem.*, Bd. **81**, 324–336. Uber die Fortpflanzungsgeschwindigkeiten kleiner schwingungen in einem unbegrenzten isotropen kreiszylinder.
13. R. BREPTA and M. PROKOPEC 1972 *Stress Waves Propagation and Impacts in Bodies*. Prague: Academia (In Czech).
14. S. WOLFRAM 1991 *Mathematica*: *a System for Doing Mathematics by Computer*. Reading, Massachusetts: Addison-Wesley; second edition.

APPENDIX A: EXACT SOLUTION FOR ROTATIONALLY SYMMETRIC WAVES IN INFINITE ISOTROPIC HOLLOW CYLINDER

As the dispersion equation acquires a very complicated form, its development, is given only as an outline without the resulting relations. The solution can be assumed in the form

$$u = U(r)\sin[\xi(x+ct)] \quad \text{or} \quad u = U(r)\,\mathrm{e}^{\mathrm{i}\xi(x+ct)},$$
$$w = W(r)\cos[\xi(x+ct)] \quad \text{or} \quad w = W(r)\,\mathrm{e}^{\mathrm{i}\xi(x+ct)}, \tag{A.1}$$

with

$$U(r) = -\frac{1}{\xi^2 c^2}\left\{c_1^2 \mathrm{i}\xi \Delta - \frac{2c_2^2}{r}\frac{\mathrm{d}}{\mathrm{d}r}[r\Omega(r)]\right\},$$

$$W(r) = -\frac{1}{\xi^2 c^2}\left[c_1^2 \frac{\mathrm{d}\Delta}{\mathrm{d}r} + \mathrm{i}2c_2^2\xi\Omega(r)\right], \tag{A.2}$$

where i is the imaginary unit, $c_1 = \sqrt{(\lambda+2G)/\rho}$ and $c_2 = \sqrt{G/\rho}$ are longitudinal and shear wavespeeds in a 3-D continuum, E is Young's modulus, G is shear modulus, $\lambda = \mu E/(1+\mu)(1-2\mu)$ is Lamé's constant and μ is the Poisson ratio. Further,

$$\Delta(r) = A\mathrm{Y}_0(\alpha r) + B\mathrm{J}_0(\alpha r),$$
$$\Omega(r) = C\mathrm{Y}_1(\beta r) + D\mathrm{J}_1(\beta r), \tag{A.3}$$

where A, B, C, D are integrating constants, Y and J are Bessel functions in the usual notation and

$$\alpha = \xi\sqrt{\frac{c^2}{c_1^2}-1}, \quad \beta = \xi\sqrt{\frac{c^2}{c_2^2}-1}. \tag{A.4}$$

The integrating constants are obtained from conditions of zero normal and shear stresses on free surfaces:

$$\sigma_{rr} = \left[\lambda\Delta(r)\mathrm{e}^{\mathrm{i}\xi(x+ct)} + 2G\frac{\partial w}{\partial r}\right]_{\substack{r=R_1\\ r=R_2}} = 0,$$
$$\tau_{rx} = G\left[\frac{\partial w}{\partial x} + \frac{\partial u}{\partial r}\right]_{\substack{r=R_1\\ r=R_2}} = 0. \tag{A.5}$$

The nullified determinant for the set of four equations (A.5) gives the dispersion equation.

APPENDIX B: ANALYTICAL SOLUTION FOR TORSIONAL WAVES IN INFINITE ISOTROPIC HOLLOW CYLINDER

The dispersion equation for torsional waves in hollow cylinder can easily be expressed by the nullified determinant

$$\det\begin{bmatrix} d_{11}, & d_{12} \\ d_{21}, & d_{22} \end{bmatrix} = 0, \tag{B.1}$$

where

$$d_{11} = \frac{\beta R_1[\mathrm{Y}_0(\beta R_1) - \mathrm{Y}_2(\beta R_1)]}{2} - \mathrm{Y}_1(\beta R_1),$$

$$d_{12} = \frac{\beta R_1[\mathrm{J}_0(\beta R_1) - \mathrm{J}_2(\beta R_1)]}{2} - \mathrm{J}_1(\beta R_1),$$

$$d_{21} = \frac{\beta R_2[\mathrm{Y}_0(\beta R_2) - \mathrm{Y}_2(\beta R_2)]}{2} - \mathrm{Y}_1(\beta R_2),$$

$$d_{22} = \frac{\beta R_2[\mathrm{J}_0(\beta R_2) - \mathrm{J}_2(\beta R_2)]}{2} - \mathrm{J}_1(\beta R_2). \tag{B.2}$$